Fest, E., Shea, K. and Smith, I.F.C. "Active Tensegrity Structure" Journal of Structural Engineering, Vol 130, No 10, 2004, pp 1454-1465.http://cedb.asce.org Copyright ASCE

An active tensegrity structure

Etienne Fest[1], Kristina Shea[2], and Ian F.C. Smith[3]

Keywords: space structures; active structure; Tension; Tests.

Abstract:

Most active structures involve the direct control of single parameters when there is a closed form relationship between required response and the control parameter. Building on a previous study of an adjustable structure, this paper describes geometric active control of a reusable tensegrity structure that has been enlarged to five modules with improved connections and equipped with actuators. Closely coupled strut and cable elements behave non-linearly (geometrically) even for small movements of the ten telescopic struts. The control criterion of maintaining upper surface slope has no closed form relationship with strut movements. The behavior of the structure is studied under 25 load cases. A newly developed stochastic search algorithm successfully identifies good control commands following computation times of up to one hour. Sequential application of the commands through sets of partial commands helps avoid exceeding limits during intermediate stages and adds robustness to the system. Reuse of a previously calculated command reduces the response time to less than one minute. Feasible storage and reuse of such commands confirm the potential for improving performance during service.

1 Introduction

Even though they were invented forty years ago (Emmerich 1964, Fuller 1962 and Snelson 1965), tensegrity structures can not be yet qualified as useable permanent structural systems. Currently, their construction is limited to creating sculptures and temporary structures for exhibitions. Giving tensegrity structures capabilities to maintain serviceability criteria may extend their usefulness. R. Buckminster Fuller, one of the inventors, described tensegrities poetically as “small islands of compression in a sea of tension”. Except for the visual metaphor explaining its rigidity principle, contemporary engineers do not agree on a universal definition of tensegrities. A controversial aspect is

[1] Res. Associate., Structural Engineering Institute, IMAC-IS-ENAC, Swiss Federal Institute of Technology 1015 Lausanne EPFL, Switzerland., etienne.fest@epfl.ch
[2] Lecturer, Cambridge University Engineering Department, Cambridge, UK, ks273@eng.cam.ac.uk
[3] Prof. M.ASCE, Structural Engineering Institute, IMAC-IS-ENAC, Swiss Federal Institute of Technology 1015 Lausanne EPFL, Switzerland., ian.smith@epfl.ch

whether compression members are allowed to join. Motro (2002) proposes a broad definition for the tensegrity state: "A tensegrity state is a stable self equilibrated state of a system containing a discontinuous set of compressed components inside a continuum of tensioned components". Since this definition includes structures where compression members join, and since buckling of compression members is often critical, more efficient structures would fall into this structural category (Robbin 1996, Wang 2002).

Tensegrities are lightweight space reticulated structures that can be easily dismantled and therefore, provide innovative possibilities for reusable and modular structures. Potential applications are temporary exhibition roofs (Pedretti 1998), radio telescopes, spatial deployable masts (Tibert 2002), air wings (Skelton et al. 2001) and space antennas. In contrast with tensile membrane structures, tensegrities self-stressing characteristic means that they do not need massive anchorages or compression rings. Nevertheless, tensegrities are recognized as being efficient structural systems (Motro 2003) and the number of full-scale prototypes built is increasing. The largest laboratory structure is a double layer grid whose rectangular configuration covers an area of 82 m^2 with a self weight of 11 kg/m^2 (Raducanu and Motro 2001). Few prototypes have been tested experimentally. Saitoh (2001), through loading a tensegrity arch, showed that its analytical model was able to correctly reflect its real behavior. Except for a few experimental studies, most of the research activity on tensegrities is focused on theoretical aspects. For example, studies have been carried out on the identification of selfstress states and infinitesimal mechanisms (Pellegrino and Calladine 1985, Vassart et al. 2000), morphology, analytical and numerical prestresseability characterization (Sultan et al. 2002), dynamic behavior (Murakami 2001), tensegrity masts (Micheletti 2001) and deployable structures (Furuya 1992, Le Saux 1999,). The tensegrity configuration even arouses the interest of biologists who use them for modeling and explaining cell shape deformations (Ingber 1998).

Tensegrities are flexible structures and are sensitive to asymmetric loads and small environmental changes. Thus, they are often governed by serviceability criteria. Adaptation by changing their selfstress states provides opportunities for meeting such criteria. Equipped with sensors and actuators, active tensegrities provide the potential to control their shape and adapt to changing tasks and environments (Shea et al. 2002). In this way, they have the potential, for example, to become a part of an exhibition rather than merely provide shelter for one. Moreover, Skelton et al. (2001) demonstrate that in contrast to classical structures, tensegrities do not need excessive quantities of energy to ensure adequate control.

Until now, most structural control research in civil engineering has focused on active control of structures in order to

enhance safety under extreme loading. While maintaining serviceability was mentioned in early work as a goal of structural control, there has been little investigation in this area (Shea et al. 2002).

Researchers have recently studied theoretically the control of tensegrity structure whose behavior is geometrically non linear and coupled. Djouadi (1998) focused on controlling the vibrations of four tensegrities modules that form a cantilever beam by changing their strut lengths. By changing strut lengths, Kanchanasatool and Williamson (2002) controlled the upper plane of a tensegrity module by linearising the dynamics of the system. Their linearized model gave a good approximation of the non linear behavior of the structure. Sultan et al. (2002) controlled the shape of a one module tensegrity structure by changing cable lengths. They were able to control the upper level height under loading using symmetrical motions based on Lagrangian dynamics.

Experimental work exploring active tensegrity potential was carried out by the authors (Fest et al. 2003) on a three module manually adjusted structure. Results contrasted with the assumption of Kanchanasatool and Williamson (2002); non linear geometrical behavior occurs for cases of i) small deflections, ii) where loads are applied to several joints and iii) when adjusting combinations of telescopic struts. Consequently, analytical simplification through superimposing strut length effects is not a reliable strategy to find an accurate control command. This work illustrated experimentally the potential for controlling a tensegrity by manually adjusting strut lengths in order to maintain the slope of the upper level of a three module adjustable tensegrity structure. Since these systems exhibit geometrically nonlinear behavior and are highly coupled, stochastic search combined with dynamic relaxation was used to produce combinations of strut adjustments.

Tensegrities are good candidates for creating active structures. Aside from the structures in this project, no active tensegrity structure has been built that does not employ a linearized model for control. This paper builds on the work given by Fest et al. (2003). The authors present in this paper a fully active tensegrity structure that is extended by two modules from the original three module configuration. The new prototype is an asymmetric configuration where two modules do not touch supports and therefore, this addition brings the prototype closer to a practical situation. The previous total surface area of 9 m^2 (three module structure) now has increased to 15 m^2, including a wider unsupported span. This paper describes the active prototype, including the actuators and sensors which are embedded in a closed control loop, and advances in joint design. A quasi-static control strategy based on stochastic search is proposed and evaluated. Through testing several load cases, the paper explores the benefits of embedding a control system in a tensegrity structure in order to satisfy a serviceability criterion.

2 Description of the tensegrity structure

The prototype was designed and built at the Applied Computing and Mechanics Laboratory (IMAC) at EPFL (Fig. 1) and was inspired by an original design by Passera & Pedretti (Pedretti 1998), for the Swiss National Exhibition. The structure consists of five modules arranged in an asymmetric configuration and contains connection module joints and as central node designs that have been improved from those presented in Fest et al. (2003). Each module contains six struts and twenty-four cables. In contrast with classical tensegrity structures, a central joint is used to reduce the buckling length of the compression members, thereby lowering the cross-sectional area required to avoid buckling of the struts. Telescopic struts, now active rather than adjustable members (Fest et al. 2003), are used to modify the geometry and self-stress in the system. Six-millimeter diameter stainless steel cables form a double-layered structure, where lateral cables connect top and bottom layers. Each layer is composed of two cable lengths, one forming three isosceles triangles and the other forming an equilateral triangle in the center, see Fig. 1.

When five modules are connected to create one tensegrity structure, the total number of joints is 51 and the number of tension and compression elements is 150. The height of the structure is 1.10 m and weights 30 kg/m^2. Mechanical properties of struts and cables were not modified with extension from three (Fest et al. 2003) to five module configuration. Six degrees of freedom are fixed at the three supports. Since the two modules in the middle are only connected to their neighboring modules and are not supported, this new configuration resembles a practical situation more closely than the three module structure (Fig. 2).

Both joint types have been improved over previous designs in order to increase stability and rigidity as well as to reduce frictional effects. Differences between measurements and the idealized structure are reduced by the following new design attributes:

- The six struts of each module meet at the central joint. This joint is composed of a lubricated steel ball that is in contact with the extremities of each strut (Fig. 3b). The other end of the strut consists of a nut/threaded rod system to erect the structure (Fest et al. 2003) using a simple wrench. Changing the strut lengths results in changing the amount of self-stress in the structure.
- In order to accommodate different connection situations between multiple cables and between cables and struts, a module-connection joint was created (Fig. 4). However, it could deform non-linearly with changing tension in the attached cables. In the new design, rings tie the joint together to limit this effect (Fig. 4b).

3 Shape control of an active tensegrity structure

3.1 Numerical modeling

The tensegrity structure is equipped with sensors and actuators such that the shape and thus the behavior of the structure can be adapted. The way that shape control is carried out is schematically summarized in Fig.5. The initial state of the structure is disturbed by a load. The structural response is then introduced as an input to the search that combines a predictive model, *the analytic model*, with the search algorithm. Response displacements, δ_i, can be predicted from structural analysis as well as by measuring the structure under loading. The model is based on the geometry, topology and material properties of the structure analyzed using the dynamic relaxation method (Barnes 1977, Rossier 1993), a non-linear analysis method, which has been shown reliable and accurate for this application (Fest et al. 2003).

The search is made considering objectives and constraints, such as slope and cable elastic limit. The search result consists of a set of strut elongation applied to the loaded structure. The new structural response is then measured to quantify the effectiveness of the shape control.

Finding a good set of adjustment commands for such a coupled, non-linear system is a complex problem. There is no closed form solution for the system; that is, the relation between inputs and outputs is not deterministic. For this reason, relating a target slope to a set of required struts lengths (Fig. 6b) is not straightforward as determining slope from given strut lengths (Fig. 6a). The process that finds a control command consists of the generating, analyzing and verifying a candidate command set.

Analyzing all theoretically possible commands is combinatorially explosive leading to an exponentially increasing number of analyses with the number of active struts. A systematic search is required to determine which strut to change length and by how much. For this tensegrity structure, there are ten active struts and the number of possible strut positions is determined by the range of movement, 50 mm, and the smallest admitted movement, 0.1 mm. This scenario results in over 9.75×10^{26} possible combinations of strut lengths. Placing constraints on the number of adjustable struts creates smaller solution spaces. As an estimate, each calculation takes 0.3 seconds. The time needed to test all possible solutions evaluates to 9.29×10^{16} centuries.

Searching large solution spaces through stochastic search methods can identify beneficial adjustment commands (Fest et al. 2003). In this previous study simulated annealing search was used. For the five module active structure described

in this paper another stochastic search method, PGSL (Probabilistic Global Search Lausanne) (Raphael and Smith 2000) will be used, as it requires tuning only three search parameters to adapt to a new search task, while simulated annealing requires more (Domer et al. 2003).

PGSL is a stochastic search algorithm based on the assumption that better sets of solutions are more likely to be found in the neighborhood of sets of good ones. Solutions are generated randomly in the search space according to a probability density function (PDF), and they are evaluated using a user defined objective function. The user specifies the initial range of values of parameters. The algorithm dynamically updates the PDF such that a more intensive search is carried out in regions containing good solutions.

3.2 Control scenarios, actuator placement and control setup

In extending the three module structure to five modules, the initial control objective of maintaining a zero slope (Fest et al. 2003) has been modified. While the symmetric configuration of the three modules permits starting from a state where all response joints are at the same height, the asymmetric configuration and deformations from dead load and actuator weight now yield unequal initial heights of the response joints.

The goal of shape adjustment in this study is to maintain the initial slope of the structure on the upper level. Joints 37, 43 and 48 are chosen to represent the upper-level slope and form a triangle as indicated in Fig. 7. The scenario also corresponds to setting the structure at a target slope and maintaining that slope. The response joints are instrumented with three linear variable differential transformers (LVDTs) to measure vertical displacements, δ_i. Nominal accuracy of LVDTs is +/- 10 microns, sensors are fixed to a rigid framework encapsulating the entire structure (Fig.8). The shape control task consists of changing the lengths of a number of the telescopic struts such that the slope is maintained from the region of the high point, PH (see Fig. 7), to the region of the low point (PL). The initial slope under dead load of the system, $slope_{initial}$ should be maintained (Fig. 9). In other words, deviation from the initial slope, $\Delta slope$ (Eq. 1), is calculated through a concatenation of the relative vertical displacements of the three joints divided by the distance between PH and PL, $L_{PH-PL} = 4600\ mm$, (Eq. 2). The $slope_{modified}$ is the slope modified by loading:

$$\Delta slope = slope_{initial} - slope_{modified} \qquad (1)$$

$$slope = \frac{\left(\delta_{43} - \frac{\delta_{48} + \delta_{37}}{2} \right)}{L_{PL\text{-}PH}} \qquad (2)$$

Maintaining the initial slope does not require that the upper layer of the structure returns to its initial position after loading. Multiple solutions can also be found either above or below this position (Fig. 9).

For the five module tensegrity, 30 telescopic struts have the potential to be adjusted. The number of active struts has been chosen to be 10, that is two jacks located symmetrically along the same axis in each module (Fig.7). Note that the system is underactuated, since 10 active struts need to deal with a system with a larger number of degree of freedom. The following aspects were considered when choosing the number of active struts and their location:

- increasing the number of active struts from two to five per module does not necessarily lead to improved performance for this structure (Fest et al. 2003);
- it is desirable for a modular structure that the same struts in each module be made active such that individual modules can be constructed uniformly and then assembled on site;
- the choice of the active struts is constrained by symmetry so that a similar arrangement should be applicable when enlarging the structure to more than five modules,;
- strut movements should lead to the maximal number of lengthening directions of the structure and the maximal coupling of the active struts;
- strut movements are possible on both the lower and the upper level;
- strut movements are not performed on the three struts that are connected to supports; and
- the three struts that are fixed to response joints are not active.

It is noteworthy to mention that placing actuators in line along a common axis also reduces the displacement of the central node (as compared with one actuator), thereby lowering an important cause of geometrical nonlinear behavior, thereby stabilizing the structure.

An actuator consists of an electromechanical jack which produces linear energy from rotary energy (Fig.10). Rotary energy is created by an electric asynchronous motor via a bevel gear system (worm and wheel) and a screw nut system. Each actuator is equipped with a LVDT to measure the displacement of the piston, which is the continuation of the screw. The LVDT is used as a feedback control sensor. In cases of unpredictable situations, the piston stroke displacement is bounded by a displacement limitator which, when touched, shuts off the motor.

To ensure a safe and rapid control system, all the devices are multiplexed on a serial bus. The CAN (Control Area

Network, Bosch 1993) bus, under CANopen protocol enables to communicate in real-time between the devices. The information is provided via a PC interface card piloted by a program written in Labview (Fig. 11). The program permits automated application of a control command. An automatic override is built into the program, which will cause the system to stand by if a maximum stroke displacement is detected by a LVDT. More detailed information of the active system configuration is given by Fest (2002).

Additional weight (400 N) and rigidity of the jack need to be added to the analytic model. While the bending deformations of the active strut associated with the dead load of the jack are very small, we considered only the unilateral rigidity on the struts. Rigidity is determined by calculating an equivalent Young's modulus of the strut considering an undeformable jack. The jack weight is distributed to the two element nodes in proportion to the position of the center of gravity to the ends of the active strut.

The nominal initial length of the struts is of 1296 mm. For these tests, a 2.5 mm pre-stress position, which corresponds to strut lengths of 1298.5 mm, is taken to be the zero position. Each active strut can then be either lengthened or shortened in discrete increments that is determined from LVDT accuracy level. In order to avoid maximum stress and critical buckling force, changes in strut length are restricted to +/- 25 mm. The allowed stress in cables, 613 MPa, against yielding incorporates a safety factor of two. The maximum compressive force in struts, 20 kN, is based on experimental tests on 1 m struts. With the new control objective, a constraint has been added. It ensures a minimum strut compressive force; thus, avoiding tension in struts. This value has been fixed to 2 kN. Moreover, considering the LVDT accuracy of measuring displacements, the minimizing process of the stochastic search (Equation 2) is stopped when achieving a threshold. This value is fixed at 4.35×10^{-4}. Note that self weight causes an initial slope of 24.57×10^{-4}.

3.3 Activation and movement strategy

Quasi-static control is based on a two step strategy:

- Split a control movement into sequence of smaller movements. Given a command consisting of a set of strut adjustments, the experimental testing procedure is described in Fig. 12. Considering a possible 25 mm strut elongation, applying a control command at once might cause instabilities due to buckling of passive struts or cable yielding. The control command is divided into parts such that no movements exceeds a maximal increment of 3.2 mm. This value is calculated using the testing safety margin.

- Apply commands sequentially until the total command is reached. Struts are moved one by one and the sequence is fixed in order to minimize the energy in the structure; thus, shortening movements are carried out prior to lengthening ones.

Since during each step, only one active strut is allowed to move, the maximal number of steps to complete the command is 80. This number is calculated by multiplying the number of active struts (two per module times five modules) by 25 and dividing by 3.2. Due to geometrical non-linearity, intermediate stages may nevertheless overstress some elements. The effect of each stage along the path is simulated in order to avoid such problems. When a simulated intermediate stage overstresses an element, the sequence is changed.

For testing a single set of hypothetical adjustments for struts A to J, the procedure is illustrated in Fig. 12. This testing procedure is an improvement to the one used with the adjustable tensegrity structure (Fest et al. 2003) due to the continuous measurement that enables one to detect intermediate states that could meet the control objective. Also, since the path is governed by minimum energy introduction to the structure, applying a command is now safer. Fractioned commands are also necessary since the movements are larger in these tests.

3.4 Load cases

This kind of tensegrity structure is more sensitive to asymmetric edge load cases than uniform or top/center load cases (Fest et al. 2003). Accordingly, loads are applied to the upper level structure edges. Twenty five load cases are considered, including single point loads and two point loads (Table 1). The loads are applied in the negative Z direction. Since geometrical non linearity and coupling effects are significant even for small structure deformations and small changes in strut length and since the goals of these tests do not include measuring the structural capacity, the maximal load magnitude applied to a single joint is limited to 1092 N. Range of load magnitudes are applied to each selected joints. Load cases were selected in order to create appropriate and comparable slopes for the different load cases (8.69, 13.04 and 16.30 $\times 10^{-4}$) and enable demonstration of the sensitivity of the reference triangle to the load positions. As shown in Table 1, the slope is most sensitive to a one point load where load is applied to joint 48 resulting in a slope response of 16.72 $\times 10^{-4}$. For each load case, the test is carried out three times. The minimum load magnitude is determined from the repeatability of the tests. Considering a maximal standard deviation of 2.17 $\times 10^{-5}$ of the measured slope among all load cases, the minimal slope created by a load case is 6.52 $\times 10^{-4}$. The factor 30 corresponds to twice the standard deviation of the three sets of measurements times a factor of 15; such factors limit

the noise for test repeatability.

4 Results

This section describes an investigation of the slope control of the structure through a comparison of experimental testing and numerical analysis. Experimental tests were carried out three times for each load case.

4.1 Correlating the predictions with measurements for the initial slope

Control commands applied to the structure are based on the predicted response calculated by dynamic relaxation. Fig. 13 indicates the initial correlation between the Δslope predicted by the analytic model and Δslope measured on the structure for each load case, calculated using Equation 3, before applying a control command. Values of correlation close to 100 % indicate that the deviation is insignificant. In Fig. 13, correlation histogram values superior to 95 % are not labeled.

$$\text{Initial correlation [\%]} = \left(1 - \left|\frac{\Delta\text{slope}_{\text{measured}} - \Delta\text{slope}_{\text{predicted}}}{\Delta\text{slope}_{\text{predicted}}}\right|\right) \times 100 \quad (3)$$

$$\text{Deviation [\%]} = 100 - \text{Initial correlation} \quad (4)$$

For single point load cases, Fig 13a shows that initial correlation is at least 78 %. Moreover, the correlation is almost uniform for different magnitude loads applied at the same location. The average deviation is insignificant with regard to the loads applied to joint 37 (5%) and is low with regard to the loads applied to joint 48 (8%-average) since they are edge loads and produce the largest displacements. It increases slightly for load applied at joint 32 (13% -average). Applying loads at joints connected with an actuator causes the largest deviations between prediction and measurements (Load cases 1 to 6- Joint 32 and Joint 26).

For double point load cases, Fig 13b shows that the initial correlation is at least 72 %. Moreover, the correlation is almost uniform for different magnitude loads applied at the same location. Although loaded joints do not belong to measured modules, the deviation is insignificant regarding the loads applied simultaneously at joints 41 and 50 (< 5%) (Load case 20 to 22). The deviation between prediction and measurement is low regarding the loads applied simultaneously at joints 39 and 48 (average 8%) (Load case 17 to 19). It increases for longitudinal and transversal load cases (joints 37 & 45 and joints 45 & 48) (average 27 % and 26 %). Comparing initial correlation for loads applied at joints 37, 48, 37 & 45 and 45 & 48, loading the Joint 45 leads to the largest deviations. Considering all load cases, it is

noteworthy that the LVDT accuracy influences slope measurement more for low load magnitudes. Moreover, correlation variation may be caused by joint friction.

4.2 Slope control

The goal of shape control can be defined as maintaining the slope of the upper level of the structure through changing combinations of strut lengths. The response of the controlled structure, as calculated by Equation 5, is used to evaluate the effectiveness of sets of strut adjustment. Data are provided by measurements on the structure. The initial slope $slope_{initial}$ is the slope under dead load of the system. The variable, $slope_{modified}$ is the slope modified by loading. The variable, $slope_{adjusted}$ is the slope modified by loading and corrected by a command determined by the search.

$$Slope\ compensation\ [\%] = \left(1 - \left| \frac{slope_{initial} - slope_{adjusted}}{slope_{initial} - slope_{modified}} \right|_{measured} \right) \times 100 \qquad (5)$$

It is noteworthy that all control commands did not require the same search time, that is execution time of PGSL, even when the search space was the same size (Fig.14). Fig. 14 illustrates the search time distributed in duration intervals. The total number of PGSL search runs is 225, i.e. each of the 25 load cases was performed nine times. The white column represents the ratio (percentage) of the number of search process completed within a time range and the total number of search processes completed in less time than the upper limit of the range. The dark column corresponds to the ratio of the accumulated number of search processes starting at time zero for a certain duration and the total number of search processes. Considering the 25 load cases, the search process was completed faster than one hour (PC 2.2 GHz/512 MB). Fig. 14 indicates that most search processes (71 %) were completed within 1 to 10 minutes, but nine search processes (4%) needed more than 30 minutes and can take almost one hour. It is important to note that search time is linked to the complexity of the control objective as well as hardware. For comparison, Shea et al (2002) have found that determining a set of adjustments for controlling the slope of a three module structure took approximatively 160 minutes (SGI octane 175MHz/128 MB).

To give a more detailed example, a command generated by the search for load case 8 is listed in Table 2. The command (last row) is divided into three fractions with a maximal shortening change of -2.45 mm for lower case strut 29 and extending change of 1.5 mm for the Strut 148. Applying the command to the structure in 30 steps, starts with shortening Strut 29 by 2.45 mm and finishes by extending Strut 148 by 1.57 mm to achieve the final length. The initial and final deformations and slope are shown in Table 3. A graphic illustration is shown in Fig. 15.

In Fig.16, values of slope compensation close to 100 % indicate that the slope of the structure has been returned to the desired slope. Slope compensation histogram values superior to 95 % are not labeled and identify good control commands. Shape control is tested for 25 load cases. Slope compensation effectiveness is shown in Fig. 16a for single load cases. Applying a control command results in changes to the upper plane enabling it to compensate at least 78% of the slope. For nine load cases out of 13, the control commands determined are good (compensation >95 % for load cases 1 to 6 and 10 to 12).

Regarding double point load cases, slope compensation effectiveness is shown in Fig. 16b. For ten load cases out of 12, the control command permits the structure to compensate for more than 86 % of the slope that was modified by loading. For seven load cases on a total of 12, the control commands applied are good (compensation >95 % for load cases 14 to 16 and 22 to 25 and 20).

Compensation effectiveness decreases for coupled load cases when the applied load magnitude is high, e.g. load cases 20 to 22. Slope compensation starts at 95 % and goes down to 76 % and finally reaches a minimum of 65 %. In these load cases, the measured joints do not belong to the loaded modules. Regarding Load case 22 (65 % compensation), the sequence in applying the command may as well alter the control. Indeed, non-linear geometrical systems are sensitive to the sequence of applied loads.

Regarding all load cases, the quasi static control strategy, consisting of dividing the command into sequences of parts, lead to no difficulties satisfying strength and buckling constraints, and it proved successful for meeting the control objectives. The analytic model, incorporating the active elements, is well suited for predicting the structure deformation. For all load cases, changing the strut lengths resulted in changes in the upper level slope toward the performance goal of restoring the initial slope. It shows that the combination of PGSL with dynamic relaxation has the potential for identifying good sets of adjustments even in situations of non-linear behavior and exponentially complex search spaces. Positioning actuators along the same line is well suited for this application. Regarding all load cases, results demonstrate that actuator positions are well suited for the structure and the control objective under study.

4.3 Robustness

In the figures, continuous lines are used to show the displacements calculated by the analytic model and dotted lines represent the slope measured. Fig. 16 has shown that good control commands exist and can be identified in order to ensure that a serviceability criteria is met. It is interesting to explore how the initial correlation between prediction and measurement could affect the quality of slope compensation.

Comparing Figs. 15a and 16a and comparing Figs. 15b and 16b, show that an initial deviation between prediction and measurement does not necessarily lead to low slope compensation after applying a control command. Regarding load cases 1 to 3, although the average initial correlation is only around 78 %, applying a control command modifies the slope and permits the structure to regain more than 95 % of the initial slope. Fig. 17a shows that applying a command by steps makes the slope converge to the initial slope, even with an initial correlation of 78 %. The vertical axes in Figure 17 are the number of Equation 5. Here, considering the changes in strut length predicted were all less than 3.2 mm, the command did not need to be factorized. In this load case, the entire command did not need to be applied since total slope compensation is achieved between steps 9 and 10. The 10^{th} fraction is only partially applied. Measuring continuously the slope and strut length during the strut adjustments makes it possible to identify when slope is completely compensated. Table 4 compares the command predicted and the command applied and measured on the structure. It shows that lengthening Strut 90 by 1.92 mm (80 % of the predicted length) instead of 2.4 is enough to compensate the slope.

Regarding load cases 23 to 25, although the average initial correlation is only around 73 %, applying a control command lead to more than 95 % recovery of the initial slope. For example, in load case 23, an initial correlation of 78 % was established between measurement and prediction. Fig. 17b shows that the command that is applied to structure step by step, enables complete compensation of the initial slope. In this load case, the entire command did not need to be applied, because full slope compensation is achieved between steps 12 and 13. The 13^{th} fraction is partially applied. Regarding the shape of the curves, some struts have a more prominent effect on the slope variation than others.

Both load cases show initial deviations between prediction and measurement that fortunately do not result in the system divergence. Such robust behavior was observed repeatedly. The incertitude does not accumulate throughout the adjustments; incremental adjustments bring the structure closer to its initial slope. For load cases where the initial correlation was below 85 % (load cases 1 to 3, 10, 11, 14 to 19, 22 to 25), the slope prediction was higher than the slope measured, i.e. the model predicts a more flexible structure than in reality. For these load cases, the control command fully compensated the slope. When the control command is calculated for a more flexible structure than the real structure, it is likely that applying this command to the real structure has a positive effect on slope compensation. Nevertheless, in cases of large initial deviations between predictions and measurements, it could be dangerous, since

real forces in members would be underestimated.

4.4 Comparing two solutions

As suggested in Fig. 9, multiple solutions exist and are found using stochastic search (Fig. 18). To investigate equivalence of predicted similar quality solutions, two solutions were tested on the structure for the load case 14. As shown in Table 5, commands are quite different. Comparing both commands, many of the struts that are adjusted are moved in opposite directions, thus, illustrating that very different solutions are possible. For instance, strut 116 should be shortened by 2.80 mm in command 1, while strut 116 should be lengthened by 0.5 in command 2. Moreover, command 1 only needs six active members while command 2 needs ten active members.

Considering slope compensation, both commands are effective and are applied only partially. Criteria that helps to choose among the two commands can be formulated. For instance, Solution 1 could be selected since it requires less energy or due to its proximity to the initial position of the struts. In summary, it is likely that for such a non-linear system, a multi criteria search would be needed for control objectives that are associated with serviceability. This research is underway.

In situations where achieving the performance goal with just one command is not completely successful, opportunities exist for making further iterations beginning with the new deformed shape. Iterative control leads to an active structure that can be modified step by step, provided that convergence is probable. Three possible strategies for iterative control are discussed.

- Strategy 1: Analyze the response of the structure to a control command in order to highlight which strut for this load case had the most influence on the slope variation. A new command is built allowing only micro-movements (+/- 1 mm) of struts starting with the most influential struts and stopping when the initial slope is regained. This technique is intended for small slope compensations associated with small strut movements. The effect of the additional commands is checked in order not to reach the material and geometrical capacities of the structure.
- Strategy 2: Use the original command and create a new one by scaling a command fraction in smaller steps. Starting at the final position resulting from the original command, parts of the command fraction are applied successively since the measurements show that the command enabled the structure to improve the slope. For instance, in load case 8, a single command enabled the structure to regain only 86 % of its initial slope. The movements of each strut are calculated by multiplying the original command by 0.15. Applying an additional

command based on the original calculated by the search algorithm enables the structure to reach maximal slope compensation (Fig. 19). Once again, the effect of the additional struts adjustments are checked in order to avoid reaching the material and geometrical capacities of the structure.

- Strategy 3: Identify a new search command with the stochastic tool starting with the deformed shape. This strategy needs a model calibration based on measurement within the search (Shea et al. 2002). Domer et al. 2003 showed the potential of improving the prediction accuracy of the three module tensegrity structure model by comparing simulations to measured data. An artificial neural network trained with these data increased the model accuracy. A technique that couples stochastic search with model calibration is currently under development in order to integrate parameters that are difficult to model, such as joint friction.

Strategies 1 and 2 proved successful for small strut length changes. However, it could be dangerous to use them in cases where there was a large slope deviation after applying the original command, due to possibilities of over stressing the structure or decreasing the slope compensation. Strategy 3 would be safer for cases where 35 % of the slope or more needs to be compensated after applying the original command. On the other hand, Strategy 3 is slower since it requires a new search. Thus, a hybrid approach would take advantage of the three strategies and would be useful for a wide range of situations.

Considering all load cases, it is likely that information about good control commands associated with prediction, iterative control and continuous measurement would be helpful in finding a control command in a similar situation loading. Good control commands and their associated sequences are stored in order to be retrieved and reused in cases where the same load case reappears. Advantages of reusing good control commands are:

- no stochastic search;
- no need to verify intermediate states associated with applying strut adjustments one by one through fractioning the command;
- less risk of iterative control when the original command is not effective enough.

For all load cases, all good control commands and their associated sequences were stored and classified in independent files with names describing the load position and its magnitude. Finding a good control command involves searching for the filename that corresponds to the load position and magnitude. Retrieving a good control command and sequence decreases the command search time to less than one minute. Considering the search time distribution given in Fig. 14, this technique has the potential to avoid search times of up to one hour. Nevertheless, in

situations where the only piece of information is the slope (unknown loads), the task is more difficult. A method for identifying loading would be necessary. Research into storing, retrieving and adapting good control commands and identifying load cases is underway. Using the control system to observe behavior resulting from small movements of active members may prove to be a good procedure for identifying loading.

5 Conclusions

Active control of a tensegrity structure results in a lightweight and reusable structural system that is capable of reacting to its environment. The challenges of creating an active tensegrity structure that satisfies serviceability criteria are threefold:

- Design and construction of an active control system for a complex structure.
- Behavior prediction of a geometrically non-linear structure with strut and cable elements as well as active members.
- Design of a control strategy for non-linear, coupled and underactuated systems that have no closed form solution for direct calculation of commands.

Results show that the control system strategy adopted in this tensegrity structure is capable of meeting a serviceability criteria. Combining stochastic search via PGSL with dynamic relaxation enables identification of good control commands to maintain the slope of the upper layer under perturbations involving asymmetric single and double vertical point loads. The quasi-static control strategy, consisting of splitting the full command into increments and applying them strut by strut with simultaneous measurements leads to a safe procedure for meeting serviceability criteria and provides opportunities to identify potentially better commands enroute to the full command. Testing has demonstrated the robustness of the system. Iterative control, starting with a deformed shape and applying an additional command, has the potential to increase control effectiveness.

Storing good control commands and their associated control sequences speeds up the search by retrieving a previous command that is associated with the same loading. Multicriteria search may be useful to find commands that, for example, provide slope compensation while maintaining the most capacity to counteract additional future loads.

This work contributes to developing a structure that, through integrating a control system, iterative control, and retrieving previous control commands, will improve its performance during service life.

6 Acknowledgments

The authors would like to thank the Swiss National Science Foundation for funding this research under contract and Maag Technic, Hi-Tech Engineering (Zurich), Lust-tec (Zurich), HBM (Darmstadt) and National Instruments for their support. We are also grateful to B. Domer, B. Raphael, Passera & Pedretti SA, S. Rossier, P. Gallay and M. Pascual and C. Gilliard for their contributions.

7 References

Barnes M.R., (1977). "Formfinding and Analysis of Tension Space Structures by Dynamic Relaxation." The City University, England.

Bosch, R. (1993). CAN Specification 2.0 Part A, pp. 31.

Djouadi S., (1998). "Le Contrôle des Structures Tensegrité et les Systèmes tensegrité." Doctoral thesis, Université Montpellier II, Laboratoire de Mécanique et Génie Civil, Montpellier, France (in French), p.134.

Domer, B., Fest, E., Lalit V., and Smith, I. F. C. (2003). "Combining the Dynamic Relaxation Method with Artificial Neural Networks to Enhance Simulation of Tensegrity Structures." *J Struct Eng-ASCE*, 129 (5), 2003.

Domer, B., Raphael, B., Shea, K., and Smith, I. F. C. (2003). "Comparing Two Stochastic Search Techniques for Structural Control." *ASCE - Computing in Civil Engineering*, to be published.

Emmerich D. G., (1964). "Construction de Réseaux Autotendants." Brevet N°1,377,290, Brevet délivré par le ministère de l'industrie, France (in French).

Fest, E., Shea, K., Domer, B., and Smith, I. F. C. (2003). "Adjustable Tensegrity Structures." *J Struc. Eng.-ASCE*, 129 (4), 515-526.

Fest, E., and Smith, I. F. C. (2002). "Deux Structures Actives de Type Tensegrité" *CTICM - Revue Construction Métallique*, 3, 19-27.

Fest, E., (2002). "Une structure active de type tensegrité. " Doctoral Thesis, Swiss Federal Institute of Technology, Lausanne, Switzerland, n°2107.

Furuya, A., (1992). "Concept of Deployable Tensegrity Structures in Space Applications" *Int. J. Space Struct.*, 7(2), 75-83

Fuller R. B., (1962). "Tensile Integrity Structures." U. S. Patent N°3,063,521.

Ingber D.E., (1998). "The Architecture of Life." *Scientific American"*, January, 30-39.

Kanchanasaratool, N., and Williamson, D. (2002). “Modelling and Control of class NSP Tensegrity Structures.” *Int. J. Control, Taylor & Francis*, 75 (2), 123-139.

Le Saux, C., Bouderbala, M., Cevaer, F., Motro, R. (1999) “*Strut-strut Contact in Numerical Modeling of Tensegrity System Folding”*, 40th Anniversary of IASS: from Recent past to Next Millenium, International Association for Shell and Spatial Structures, D1-D10

Micheletti, A., (2003) “The indeterminacy Condition for Tensegrity Towers” *Revue Française du Génie Civil, Edition Spéciale*: "Tensegrité: Analyse et Progrès", To be published.

Motro R., and Raducanu V. (2001). “Tensegrity Systems and Tensile Structures.” *Extended Abstracts International Symposium on Theory, Design and Realization of Shell and Spatial Structures*, H. Kunieda, Nagoya, 314-315.

Motro, R. (2002). “Tensegrity: the State of the Art.” 5th International Conference on Space Structures, Ed. G. A.R. Parke, P. Disney, Thomas Teldford, London, 97-106.

Motro, R. (2003). “Tensegrité: Principe Structural.” *Revue Française du Génie Civil, Edition Spéciale*: "Tensegrité: Analyse et Progrès", To be published.

Murakami, H. (2001). “Static and Dynamic Analyses of Tensegrity Structures. Part 1. Nonlinear Equations of Motion.” *Int. J Solids. Struct*., 38 (50), 3599-3613.

Pedretti M., (1998). <*http://www.ppeng.ch/base_expo.htm*> *(July. 15, 2001)*

Pellegrino S., and Calladine C. R., (1986*).* “Matrix Analysis of Statically and Kinematically Indeterminate Frameworks.” *Int. J. Solids Structures*, 22(4), 409-428.

Radacanu, V., and Motro, R. (2001). “New Tensegrity Grids.” International Association for Shell and Spatial Structures Symposium 2001, ed. Kuneida, Nagoya, 320-321.

Robbin J. L., (1996)., *Engineering A New Architecture*, Yale University Press, Princeton, 25-37.

Rossier S., (1993). “Optimization of cable structures using genetic algorithms.” *Internal report*, Swiss Federal Institute of Technology , Switzerland.

Saitoh, M., Okada, A., and Tabata, H. (2001). “Study on the Structural Characteristics of Tensegric Truss Arch.” International Association for Shell and Spatial Structures Symposium 2001, Nagoya, Ed. Kunieda, 326-327.

Shea K., Fest E., and Smith I. F. C., (2002). “Developing intelligent tensegrity structures with stochastic search.” *Advanced Engineering Informatics*, Elsevier, 16(1).

Skelton, R. E., Helton, J. W., Adhikari, R., Pinaud, J. P., and Chan, W. (2001). “An Introduction to the Mechanics of Tensegrity Structures.” Handbook on Mechanical Systems Design, 1-141.

Skelton R.E., Pinaud J.P., and Mingori D.L., (2001). “Dynamics of the Shell Class of Tensegrity Structures.” *J. of the Franklin Institute*, 338, 255-338.

Snelson K., (1965). “Continuous Tension, Discontinuous Compression Structures.” U.S. Patent N°3,169,611.

Sultan, C., Corless, M., and Skelton, R. E. (2002). “Symmetrical Reconfiguration of Tensegrity Structures.” *Int. J. Solids Struct*., Pergamon, 39, 2215-2234.

Tibert G., (2002).”Deployable Tensegrity Structures for Space Applications”, PhD, Royal Institute of Technology, Department of Mechanics, Stockholm.

Vassart N. , Laporte R. , and Motro R., (2000). “Determination of Mechanism's Order for Kinematically and Statically Indetermined Systems.” *Int. J. of Solids and Structures*, 37, 3807-3839.

Wang, B.-B. (2002). “AP & ATP Grids - Bridging Tensegrity to Cable-Strut.” 5th International Conference on Space Structures, Ed. G. A.R. Parke, P. Disney, Thomas Teldford, London, 5, 1200-1208.

Load case type	Loaded joint number	Load [N]	Module number	Simulated slope [10^{-4}]	Actuator connected
SINGLE POINT LOAD					
1- Central	26	625	1 and 2	-8.98	yes
2- Central	26	900	1 and 2	-12.61	yes
3- Central	26	1209	1 and 2	-16.52	yes
4- Central	32	625	3 and 5	-9.50	yes
5- Central	32	859	3 and 5	-12.98	yes
6- Central	32	1092	3 and 5	-16.37	yes
7- Asymétric	37	391	1	-9.06	no
8- Asymétric	37	550	1	-12.80	no
9- Asymétric	37	700	1	16.35	no
10- Asymétric	48	391	4	-9.3	no
11- Asymétric	48	550	4	-13.11	no
12- Asymétric	48	700	4	-16.72	no
13- Central	6	1092	1 and 4	-9.00	no
TWO POINT LOADS					
14- Longitudinal	37 and 45	391	1 and 3	-8.35	no
15- Longitudinal	37 and 45	624	1 and 3	-13.20	no
16- Longitudinal	37 and 45	742	1 and 3	-15.63	no
17- Asymétric	39 and 48	157	1 and 4	9.24	no
18- Asymétric	39 and 48	215	1 and 4	12.67	no
19- Asymétric	39 and 48	274	1 and 4	16.15	no
20- Coupling	41 and 50	391	2 and 5	8.63	no
21- Coupling	41 and 50	624	2 and 5	13.37	no
22- Coupling	41 and 50	742	2 and 5	15.63	no
23- Transversal	45 and 48	391	3 and 4	-8.61	no
24- Transversal	45 and 48	624	3 and 4	-13.61	no
25- Transversal	45 and 48	742	3 and 4	-16.11	no

Table 1: Load cases

Strut number	29	57	119	145	90	26	60	116	87	148
Step	1	2	3	4	5	6	7	8	9	10
Command fraction 1 [mm]	-2.45	-2.21	-2.12	-1.48	-0.9	-0.87	0.8	1.16	1.45	1.57
Step	11	12	13	14	15	16	17	18	19	20
Command fraction 2 [mm]	-4.9	-4.42	-4.25	-2.96	-1.8	-1.75	1.6	2.32	2.9	3.14
Step	21	22	23	24	25	26	27	28	29	30
Entire command [mm]	-7.35	-6.63	-6.54	-4.44	-2.7	2.61	2.4	3.49	4.35	4.71

Table 2: Sequence example of a command divided in three fractions, Load case 8

Intial slope [10^{-4}]	Modified state				Compensated state				Slope compensation (%)
	Joint height,δ [mm]			Slope [10^{-4}]	Joint height,δ [mm]			Slope [10^{-4}]	
	37	48	43 PH		37	48	43 PH		
24.57	498.8	500.6	516.9	37.39	506.5	500.1	514.6	24.56	99

Table 3: Structure deformation and slope for the command given in Table 2

Strut number	26	119	29	116	60	148	87	145	57	90
Step	1	2	3	4	5	6	7	8	9	10
Command predicted [mm]	-2.7	-2	-1.5	0.9	0.3	0.6	0.8	0.9	1	2.4
Command applied [mm]	-2.67	-1.96	-1.46	-0.86	0.26	0.56	0.77	0.87	0.93	1.92

Table 4: Comparison of command predicted, and applied (and measured), Load case 15

Strut number	116	26	119	26	145	87				
Step	1	2	3	4	5	6				
Command 1 [mm]	-2.80	-2.47	-1.15	1.35	1.58	1.86				
Strut number	26	29	145	60	119	57	87	116	90	148
Step	1	2	3	4	5	6	7	8	9	10
Command 2 [mm]	-3	-2.9	-2.9	-2.6	-2.1	-1.6	-0.5	0.5	1.1	1.5

Table 5: Two different equivalent quality commands, load case n°14

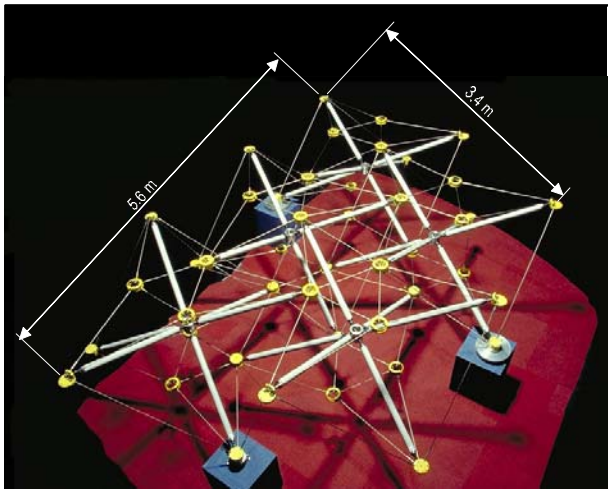

Figure 1: Picture of the five modules without actuators showing the three supports. Note that between modules, compression elements do not touch, that two modules are not supported and that the configuration is asymmetric.

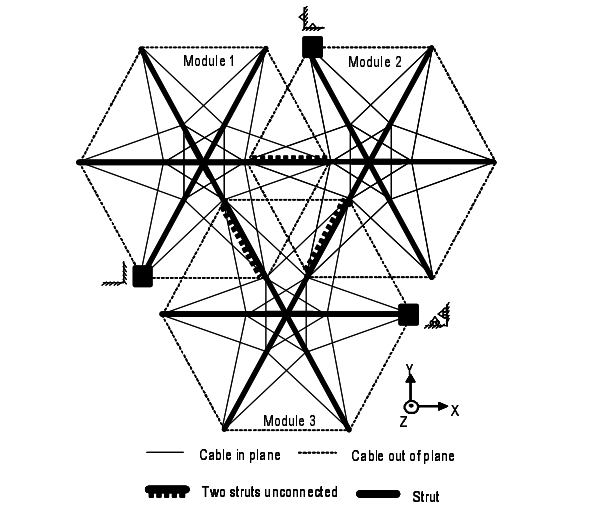

a)

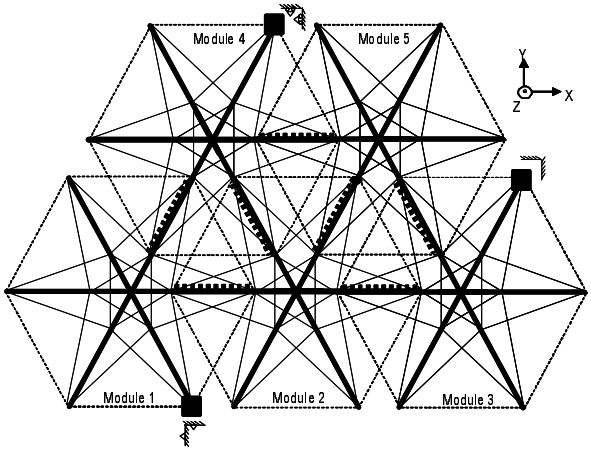

b)

Figure 2: Plan view: (a) three module structure— symmetric configuration (Fest et al. 2003), (b) five module structure— asymmetric configuration, note that Module 2 and Module 5 are not supported.

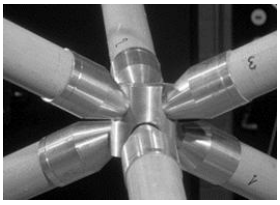

a)

b)

Figure 3: Two stages of the central joint development: (a) three module structure central joint (Fest et al. 2003) and (b) five module structure central joint

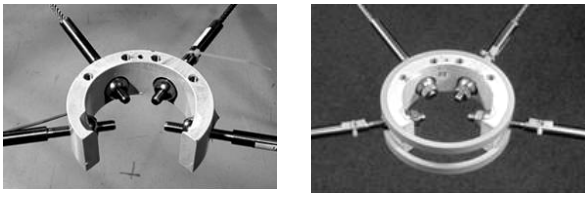

a) b)

Figure 4: Two stages of the connection module joint: (a) three module structure open ring (Fest et al. 2003) and (b) five module structure closed ring

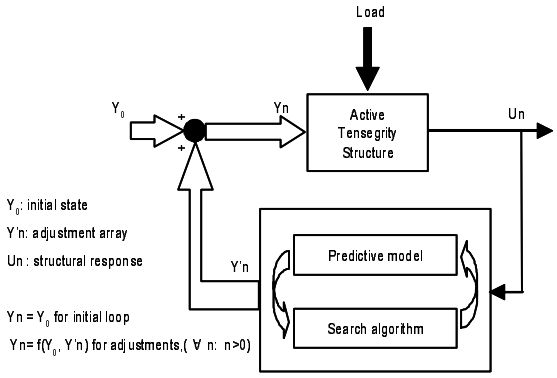

Figure 5: Shape control loop (Fest et al. 2003)

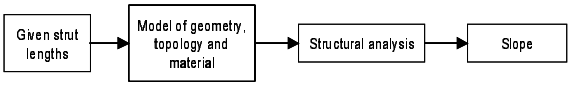

a)

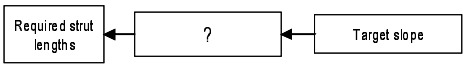

b)

Figure 6: Relations between the length of the telescopic members and the structure shape: (a) transformation from given structural geometry to slope (b) transformation from target slope to required structural geometry.

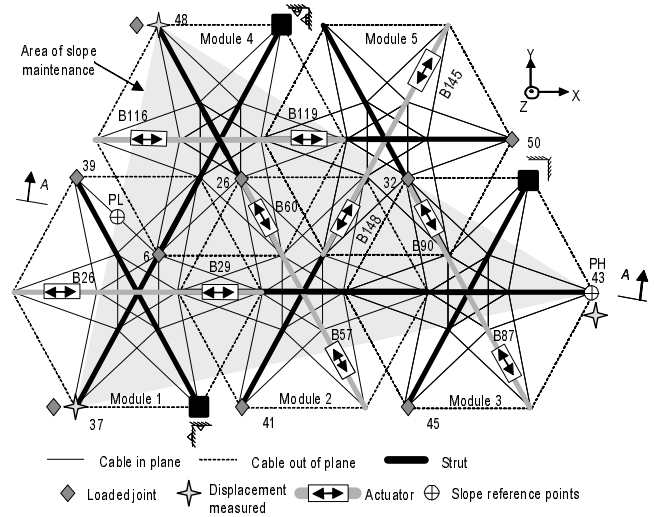

a)

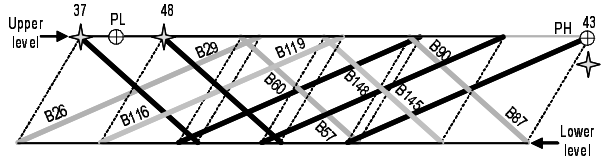

b)

Figure 7: Schematic structure view: (a) plane view of sensor, load and the control area location and elevation view of sensor, load, level and slope reference joint location

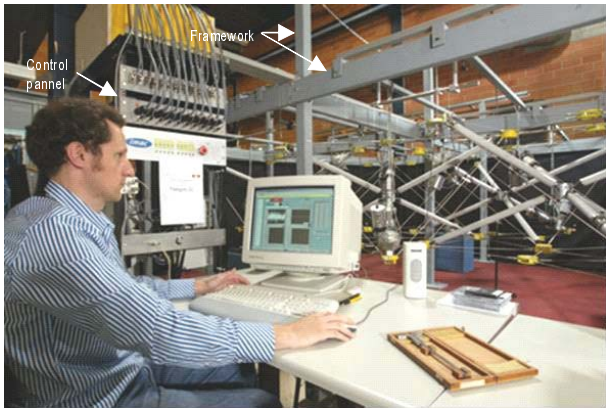

Figure 8: Global view of the entire active control system

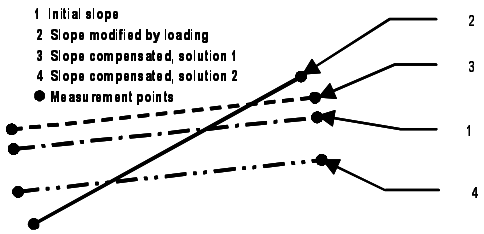

Figure 9: A two-dimensional schema of slope maintenance: the view A-A (Fig. 7).

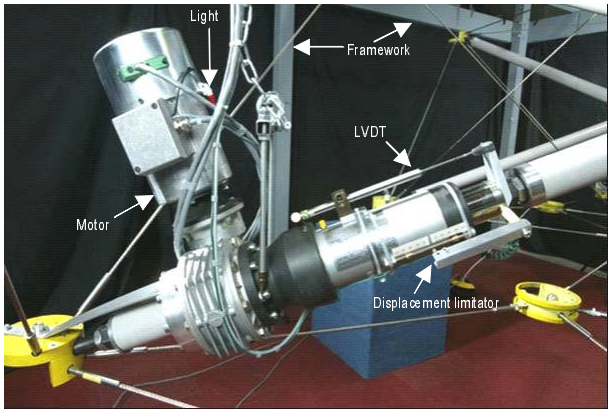

Figure 10: Elevation view of an actuator set in a strut. Note the LVDT and the displacement limitator

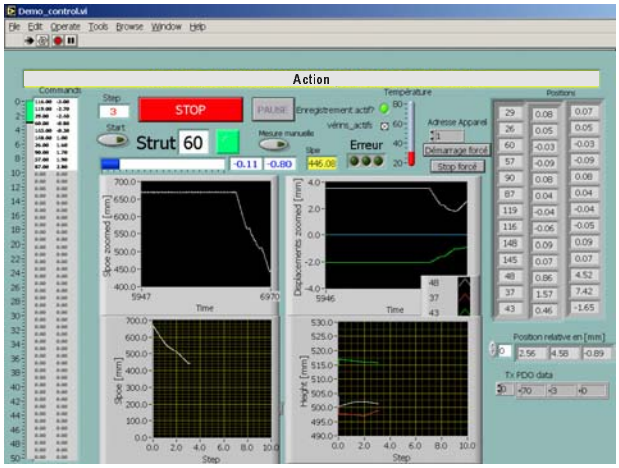

Figure 11: Control front panel

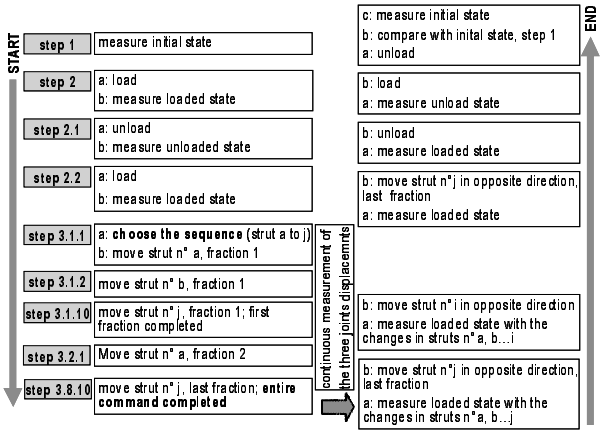

Figure 12: Testing procedure

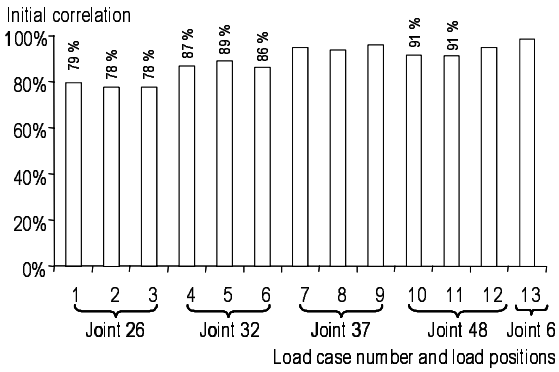

a)

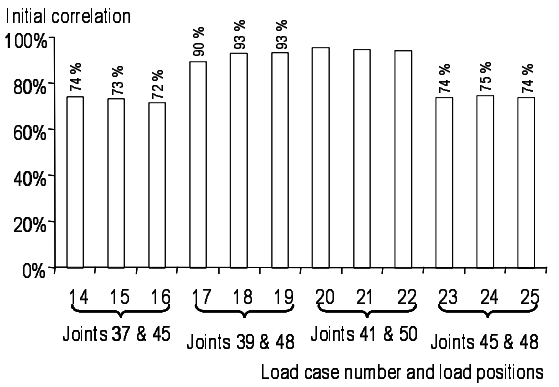

b)

Figure 13: Correlation between the predicted and measured slope due to : (a) the single load cases and (b) the double load cases

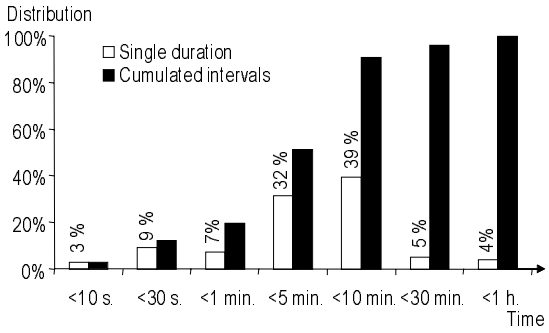

Figure 14: Distribution of the search time in duration intervals

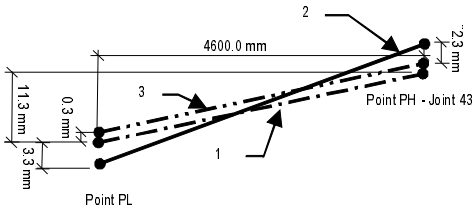

Figure 15: Displacements and slope compensation for Load case 8: view A-A, longitudinal to the control line

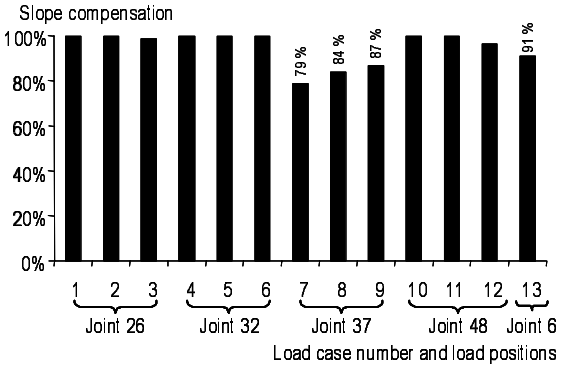

a)

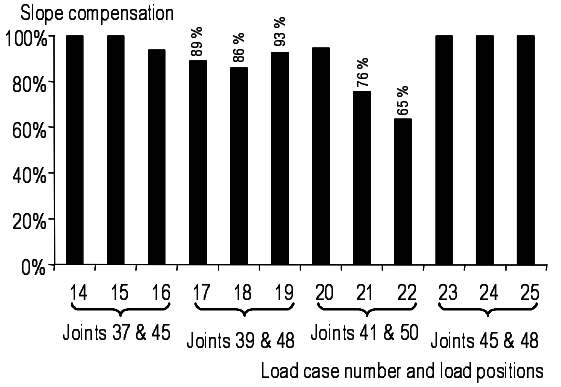

b)

Figure 16: Slope compensation: (a) single load cases and (b) double load cases

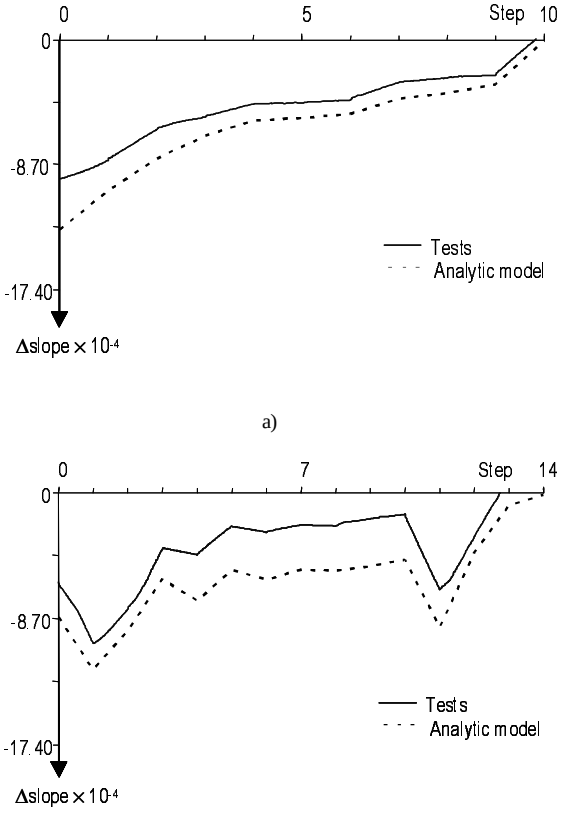

Figure 17: Prediction and measurement: of Δslope (Eq. 1) with iteration step : (a) single point load, Load case 15 and, (b) double point load, Load case 23

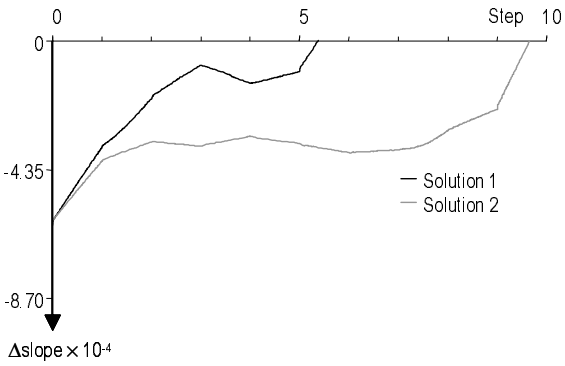

Figure 18: Slope compensation evolution comparison between two equivalent quality solutions, load case n°14

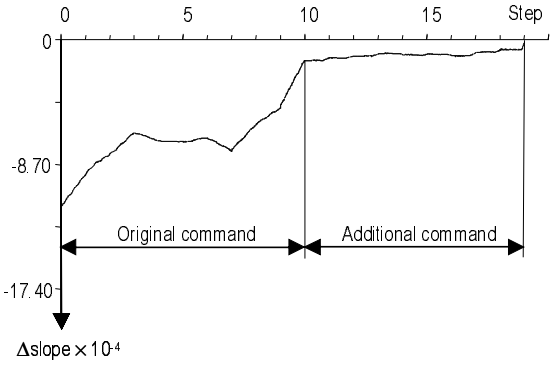

Figure 19: Iterative slope compensation, load case 8

Table 1: Load cases

Table 2: Sequence example of a command divided in three fractions, Load case 8

Table 3: Structure deformation and slope for the command given in Table 2

Table 4: Comparison of command predicted, and applied (and measured), Load case 15

Table 5: Two different equivalent quality commands, Load case n°14

Figure 1: Picture of the five modules without actuators showing the three supports. Note that between modules, compression elements do not touch, that two modules are not supported and that the configuration is asymmetric.

Figure 2: Plan view: (a) three module structure— symmetric configuration (Fest et al. 2003), (b) five module structure— asymmetric configuration, note that Module 2 and Module 5 are not supported.

Figure 3: Two stages of the central joint development: (a) three module structure central joint (Fest et al. 2003) and (b) five module structure central joint

Figure 4: Two stages of the connection module joint: (a) three module structure open ring (Fest et al. 2003) and (b) five module structure closed ring

Figure 5: Shape control loop (Fest et al. 2003)

Figure 6: Relations between the length of the telescopic members and the structure shape: (a) transformation from given structural geometry to slope (b) transformation from target slope to required structural geometry.

Figure 7: Schematic structure view: (a) plane view of sensor, load and the control area location and elevation view of sensor, load, level and slope reference joint location

Figure 8: Global view of the entire active control system

Figure 9: A two-dimensional schema of slope maintenance: the view A-A (Fig. 7).

Figure 10: Elevation view of an actuator set in a strut. Note the LVDT and the displacement limitator

Figure 11: Control front panel

Figure 12: Testing procedure

Figure 13: Correlation between the predicted and measured slope due to : (a) the single load cases and (b) the double load cases

Figure 14: Distribution of the search time in duration intervals

Figure 15: Displacements and slope compensation for Load case 8: view A-A, longitudinal to the control line

Figure 16: Slope compensation: (a) single load cases and (b) double load cases

Figure 17: Prediction and measurement: of Δslope (Eq. 1) with iteration step : (a) single point load, Load case 15 and, (b) double point load, Load case 23

Figure 18: Slope compensation evolution comparison between two equivalent quality solutions, load case n°14

Figure 19: Iterative slope compensation, load case 8